Molecular Crystals and Liquid Crystals Science and Technology. Section A. Molecular Crystals and Liquid Crystals

Publication details, including instructions for authors and subscription information:
http://www.tandfonline.com/loi/gmcl19

A Macroscopic Approach to the Light-Induced Instability of Cooperative Photo-Switchable Systems

François Varret [a], Kamel Boukheddaden [a], Jelena Jeftic [a] & Olivier Roubeau [a]

[a] Laboratoire de Magnétisme et d'Optique, CNRS-Université de Versailles, 45 Avenue des Etats-Unis, 78035, Versailles, Cedex, FRANCE

Version of record first published: 24 Sep 2006

To cite this article: François Varret, Kamel Boukheddaden, Jelena Jeftic & Olivier Roubeau (1999): A Macroscopic Approach to the Light-Induced Instability of Cooperative Photo-Switchable Systems, Molecular Crystals and Liquid Crystals Science and Technology. Section A. Molecular Crystals and Liquid Crystals, 335:1, 561-572

To link to this article: http://dx.doi.org/10.1080/10587259908028897

Mol. Cryst. and Liq. Cryst., 1999, Vol. 335, pp. 561-572
Reprints available directly from the publisher
Photocopying permitted by license only

A Macroscopic Approach to the Light-Induced Instability of Cooperative Photo-Switchable Systems

FRANÇOIS VARRET, KAMEL BOUKHEDDADEN, JELENA JEFTIC and OLIVIER ROUBEAU

Laboratoire de Magnétisme et d'Optique, CNRS-Université de Versailles, 45 Avenue des Etats-Unis, 78035 Versailles Cedex, FRANCE

Under permanent irradiation cooperative photo-switchable systems may undergo a light-induced instability of the steady state leading to thermal and optical hystereses [1,2]. We report on a non-linear macroscopic master equation which accounts for the competition between a constant photo-excitation and a self-accelerated thermal relaxation process. The equilibrium phase diagram is drawn and the instability is discussed in terms of spinodes and demixtion. Data are from the spin-crossover series $[Fe_xCo_{1-x}(btr)_2(NCS)_2].H_2O$ (noted [x=]).

Keywords: photoexcitation; cooperativity; instability; hysteresis; demixtion

INTRODUCTION

Spin-crossover solids are text-book examples of photo-excitable materials[3], usually having a low spin (LS) ground state. The optical switching is performed at low temperatures, by the so-called direct or inverse LIESST effect (Light Induced Excited Spin State Trapping[4]), using different wavelengths for the back and forth processes (red and blue/green light respectively). At higher temperatures the metastable high spin (HS) state (after photoexcitation) decays through a radiationless process[5] , i.e. the HS $\rightarrow$ LS relaxation occurs.

Recent experiments[1,2] combining photoexcitation and relaxation showed light-induced hysteresis loops. The macroscopic model[2] which explains the light-induced bistability is based on the concept of cooperative relaxation[7], an effect evidenced by the typical sigmoidal shape of the relaxation curve[7,8], i.e. the time dependence of the photo-excited fraction, $n_{HS}(t)$, after photoexcitation, is « self-accelerated ». We develop here the macroscopic model, and we investigate the phase diagram of the dynamical equilibrium and the spinodal instability. The description applies as well to any solid containing photoswitchable units, with L, H respectively standing for the stable and metastable states of the unit.

I. The self-accelerated relaxation

Cooperative relaxation involves an energy barrier $E_a(n)$ depending on the relative population, n, of the metastable state[8]. Experiments suggest a linear dependence and the relaxation rate of a thermally activated process is written :

$$k_{HL}(T,n) = k_{\infty}\exp(-\frac{Ea(n)}{kT}) = k_{\infty}\exp(-\frac{Ea(0)}{kT})\exp(-\alpha(T)n) \qquad (1)$$

where the self-acceleration factor $\alpha(T)=Ax/T$ is proportional to the inverse temperature, the strength of interactions and the atomic concentration x in the active element (in mean-field approach). The linear dependence $E_a(n)$ is correlated to a linear variation of the electronic energy gap $\Delta(n)$ in the mean-field approach. The « moving » configurational diagram is shown in Fig. 1.

II. The macroscopic master equation

Irradiation competes with the thermal H→L relaxation and, neglecting the reverse (L→H) relaxation, the master (evolution) equation of the system is :

$$\frac{dn}{dt} = \Phi_{up} - \Phi_{down} = I_0\sigma(1-n) - nk_{\infty}\exp(-\frac{Ea(0)}{kT})\exp(-\alpha(T,x)n) \qquad (2)$$

where Φ_{up}, Φ_{down} are the flows up and down, I_0 is the beam intensity, $I_0\sigma$ the probability per time unit for a molecular unit to switch L→H, and σ the absorption cross section.

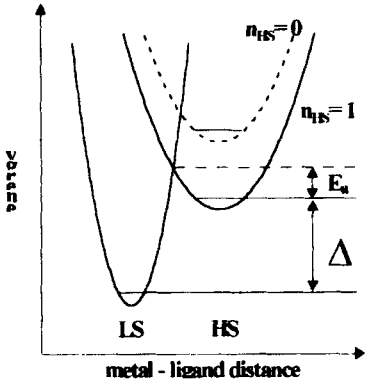

FIGURE 1 : Configurational diagram for spin-crossover, adapted from[8].

III. The steady states and the state equation

The steady state of the system (dynamical equilibrium) occurs when Φ_{up}, Φ_{down} are set equal, leading to following STATE EQUATION :

$$nk_{\infty}\exp(-\frac{E_a(0)}{kT})\exp(-\alpha(T,x)n) = I_0\sigma(1-n) \qquad (3)$$

Eq.(3) is described graphically in Fig.2, where the number of intersects is governed by the shape of $\Phi_{down}(n)$, i.e. by the α-value. It turns out :

for $\alpha < \alpha_c = 4$, there is a single solution, which is a continuous function of $I_0\sigma$ and T;

for $\alpha > \alpha_c$: a 3-state situation may occur, according to the slope of the straight line, i.e. to the value of I_0. The bistability of the system results in thermal (at I_0=constant) and optical (at T=constant) hystereses, respectively denoted : LITH/LIOH, i.e. Light-Induced Thermal/Optical Hysteresis[1, 2].

The stability character of the steady states is shown in Fig.3, through the time dependence of the system for various initial states.

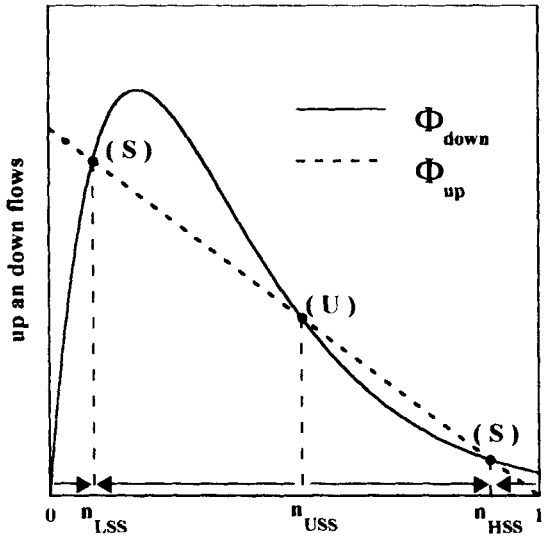

FIGURE 2 : Graphical resolution of Eq.(3) computed with α = 5.83. The steady state values are given by the intersects of the curve and the straight line. n_{LSS}, n_{USS}, n_{HSS}, respectively stand for low, unstable, high steady states.

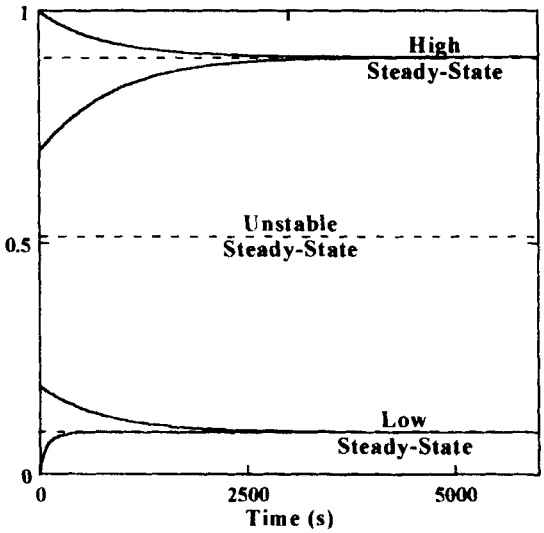

FIGURE 3 : Computed time dependence of n(t), for different initial states, with parameter values of Fig. 2.

IV. Observation of the LITH/LIOH loops (details are given in[2,9])

The LS ↔ HS switching is easily detected by magnetic measurements (for Fe^{II}, the spin states are 0, 2), or by reflectivity, or by both simultaneously[6]. Experiments were made on $[Fe_xCo_{1-x}(btr)_2(NCS)_2].H_2O$, x=0.30, 0.50, 0.85 in thin samples (~0.1 mg/mm^2). Here we show selected data for [x=0.5].

In Fig.4, the LITH loop originates from optical data which do not display the « kinetic » low-temperature tail[9] . In Fig.5 the LIOH loop was recorded according to a stepwise variation in intensities which provided data corrected from the influence of the kinetic effect. The theoretical loops on both figures (solid line curves) were computed using the value αT=265 K derived from the relaxation curves[2,9], and provide an excellent agreement with the data. On both figures the spinodes are shown by circles (see Sec. V).

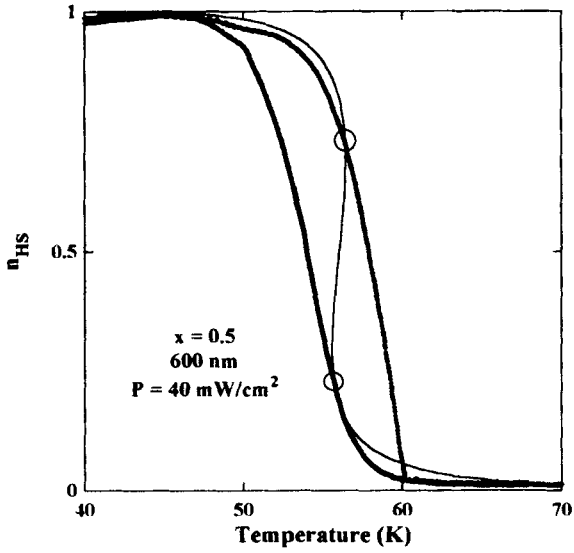

FIGURE 4 : Typical Light Induced Thermal Hysteresis loop, from optical data[2]. The solid line is computed with Eq. (3).

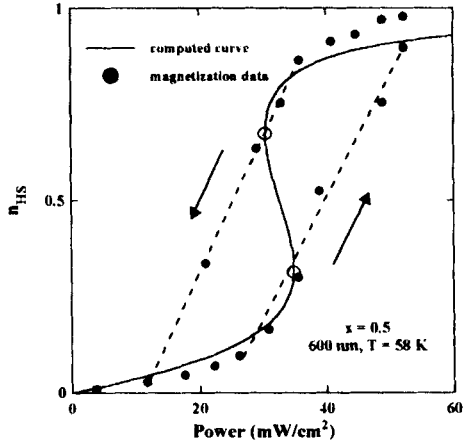

FIGURE 5 :Light Induced Optical Hysteresis loop, with computed curve.

V. Inhomogeneities and demixtion

The presence of instability induces demixtion[11]. The non-linear term in the macroscopic master equation is the driving force for the enhancement of n-value inhomogeneities in the sample. Such inhomogeneities can occur spontaneously; due to the thermal fluctuations, or result from an inhomogeneous thermo-optical treatment of the sample. Inhomogeneities in the n-values are unstable in the spinodal interval, i.e. in the range limited by the spinodes $\tilde{n}$ ', $\tilde{n}$ '', defined by the extrema of the total flow $\Phi(n) = \Phi_{up} - \Phi_{down}$.

This behaviour is due to the non-linear relaxation, see Fig.6. Indeed the evolution of the system is represented by the motion of a point of coordinate n along the n-axis, at the velocity dn/dt =Φ, which is the ordinate in the figure. Opposite motions are possible, according to the initial state of the system, as shown by arrows. In the spinodal interval, the situation is such that the more advanced the motion, the larger the velocity. This is a dispersive effect, which results in an enhancement of the inhomogeneities in the n-values. Beyond the spinodal point, the inhomogeneities are damped out. So, the inhomogeneities

transiently increase on approaching the spinodes. The effect is referred to as «spinodal instability », and vanishes below a threshold value $\tilde{\alpha}_c(I_0\sigma/k_\alpha)$, such that $\tilde{n}'$ reaches the limiting value 1. When the initial inhomogeneities extend on both sides of the instability point, demixtion can occur. An open problem is the magnitude of the correlation length (neutron diffraction data are needed).

The spinodal description includes the pure relaxation process ($I_0 = 0$) for which the transient instability is expected for $\tilde{n}' < n \leq 1$. The threshold value is then $\tilde{\alpha}_c(I_0 = 0) = 1$. The occurrence of inhomogeneities during the relaxation process results in a typical distortion of the n(t) curve, which becomes an envelop of sigmoidal curves, and develops a tail as shown in[2,9].

Optical inhomogeneities may explain the distortion of the LIOH loop in Fig.5 (see[9]) and patterns recently observed during relaxation (see[10]).

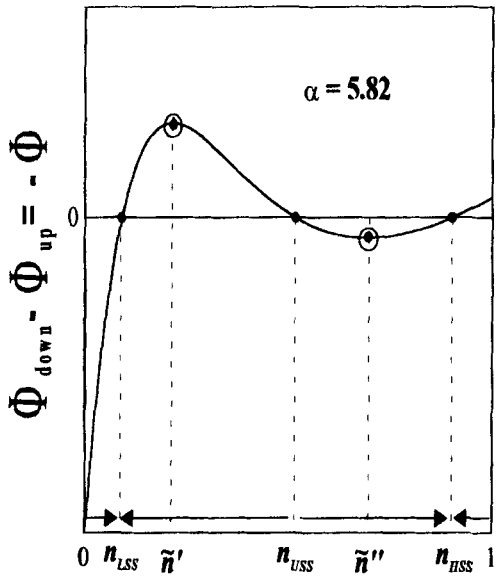

FIGURE 6 : The driving force for inhomogeneity enhancement, $\alpha=0.52 > \alpha_C$. Circles stand for the spinodes $\tilde{n}', \tilde{n}''$. Arrows show the possible evolutions.

VI. The phase diagram

In reduced variables $\theta=kT/E_a(1/2)$, $i=I_0\sigma/k_\alpha$ the state equation (3) is written

$$i(\theta,n)=\frac{n}{1-n}\exp-\frac{1}{\theta}\left[1+b(n-1/2)\right] \qquad (4)$$

where $b = \alpha\ \theta = (E_a(1)-E_a(0))/E_a(1/2)$ is the relative increase in the barrier energy. The reduced phase diagram only depends on the b-value (allowed interval from 0 to 2). Selected phase diagrams are plotted in Figs.7, 8.

The phase diagram of the non-cooperative case (b=0) is shown in Fig.7. It is reminiscent of that of a paramagnet in (T,B,M) axes.

In the cooperative case, Fig.8 shows that the surface exhibits a typical fold revealing the hysteretic character. The larger the b-value, the more extended the hysteretic region. In this figure, only the stable steady states have been represented. The unstable states are suggested by their limiting curve, i.e. the locus of the spinodal points at equilibrium, (the circles in Figs.4,5). This actually is the limiting curve of the hysteresis loops, which was derived analytically, and plotted in Figs.8, 9.

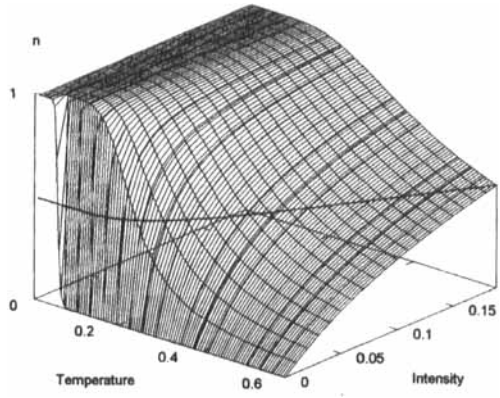

FIGURE 7 Phase diagram of the non-cooperative case (b =0), in (θ, i, n) units. Sets of curves are : iso-θ - and iso-i lines; iso-n line for n=0.5.

For all b-values, the surface includes the n-axis segment from 0 to 1 and the curve n = 1/2; i=exp(-1/θ). When projected on the T, I_0 plane, the limiting curve has a terminal point : n=1/2, i=exp(-4/b), θ=b/4, similar to the critical point of a fluid.

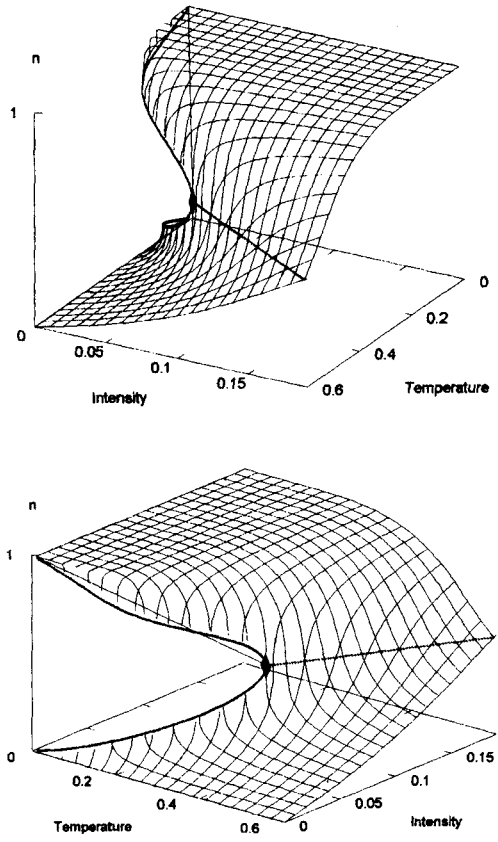

FIGURE 8 Phase diagram for the cooperative case, b =1.5, with the stable states, the limiting curve of the hysteresis loops and its terminal point (◆).

The projection of the limiting curve in the intensity-temperature plane provides the width of the LIOH, LITH loops. On increasing the temperature or the intensity, the width of the loops rises to a maximum and then decreases until the loop vanishes at the terminal point.

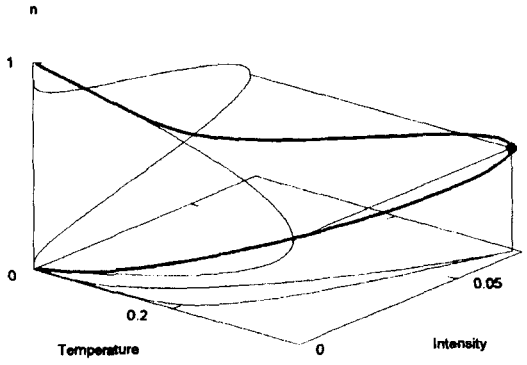

FIGURE 9 The limiting curve of the hysteresis loops, its 3 projections, b=1.5.

VII The spinodal instability volume

Spinodal points have been defined at the dynamical equilibrium, as the limiting points of the LITH/LIOH loops, and in the transient regimes, as the limiting points of a region of the state space, unstable with respect to n-value fluctuations. The latter definition is more general and includes the former as a particular case. The spinodal instability volume is made up of all the spinodal intervals [$\tilde{n}$', $\tilde{n}$''](I_0,T); it is limited by the surface $\tilde{n}$'(I_0,T), $\tilde{n}$''(I_0,T), which contains the limiting curve of the hysteresis loops. The equation of the surface is obtained by setting $\partial\phi/\partial n=0$. Then :

$$i(\theta,n) = (\frac{n\beta}{\theta} - 1)\exp - \frac{1}{\theta}\left[1 + b(n - 1/2)\right] \qquad (5)$$

The surface is shown in Fig.10. It intersects the plane i=0 on the straight line $n=b/\theta$, and the plane n=1 on a S-shaped curve. The spinodal instability volume is also limited by the planes n=1 and i=0, due to the physical restrictions $i>0$, $0 \leq n \leq 1$. At the end point : n=1, $\theta=b$, i=0, $\alpha=\alpha_c=1$.

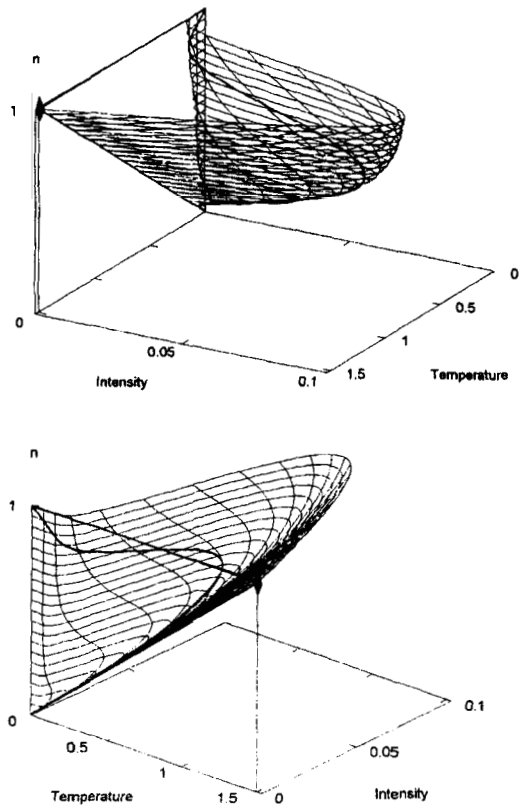

FIGURE 10 The spinodal instability volume, b=1.5, same view angles as in Fig.8. Sets of curves are : iso-θ and iso-n lines. Limiting curve of the hysteresis loops (thick line). Intersection of the planes which also limit the spinodal instability volume (thick straight line). End point (◆).

Conclusion :

Light-induced instability has been described in terms of a L→H photoexcitation in competition with the H→L cooperative relaxation. The model explains all data obtained so far in the thermal activation domain. A more complete model, presently being studied, includes a tunneling mechanism. On the other hand, the cooperative effect might not be restricted to the relaxation of the metastable state, and should be considered in relation to the photo-excitation process itself. This is a further interesting problem.

In addition, light-induced instabilities will no doubt give rise to spectacular patterns in materials under the influence of continuous excitation. Here, the explanation will require taking into account the spatial structure of the photoexcitation.

Acknowledgements
The work was supported by Centre National de la Recherche Scientifique (LMOV is Unité associée URA-1531), the Swiss National Science Foundation (for a post-doctotal grant) and European Communities for a TMR program (Contract TOSS, ERB-FMRX-CT98-0199) and for a COST Action (n°518).

References

[1] J.F. Letard, O. Kahn et al., *Inorg. Chem.* **37** 4432 (1998).

[2] A. Desaix, F. Varret et al., *Europ. Phys. Journal B inpress. Vol.6 n°2.*

[3] P. Gütlich, *Struct. Bonding* (Berlin) **44,** 83 (1981); H.Toftlund, *Coord. Chem. Rev* **94,** 67 (1989); E. König, *Struct. Bonding* (Berlin) **76,** 51 (1991); O. Kahn, *Molecular Magnetism* (VCH, New-York 1993).

[4] S. Decurtins, P. Gütlich, C. P. Köhler, H. Spiering, A. Hauser, *Chem. Phys. Letters,* **1,** 139 (1984); P. Gütlich, A. Hauser, H. Spiering, *Angew Chem. Int. Ed. Engl.,* **33,** 2024 (1994).

[5] A. Hauser, *Comments on Inorg. Chem.,* **17,** 17 (1995).

[6] F.Varret et al., *ICAME'97 (Intern. Conf. Applic. Mössbauer Affect, Rio de Janeiro Brésil, Sept. 1997), Hyperf. Inter.* **113,** 37 (1998).

[7] H. Spiering, E. Meissner, H. Köppen. E. W. Muller, P. Gütlich, Chem. Phys., **68,** 65 (1982); A.Hauser, *J. Chem. Phys.,* **94,** 2741 (1991).

[8] J. Jeftic, A. Hauser, *J. Phys. Chem. B,* **101,** 10262 (1997).

[9] O. Roubeau et al, E. Codjovi et al, *this conference.*

[10] J. Jeftic et al, *this conference.*

[11] J. W. Cahn, *Trans. Metallurgical Society AIME* **242,** 166 (1968).